Chapter 6

Some Indicators of Interannual Rainfall Variability in Patagonia (Argentina)

Marcela Hebe González

Additional information is available at the end of the chapter

http://dx.doi.org/10.5772/55494

1. Introduction

Argentina is located in the southeastern continental extreme of South America. The Andes Mountain Range extends 7240km all along the western region of the country with a mean height of 3660m above mean sea level (a.m.s.l.). Two topographical regions can be distinguished in the country: north of 40°S, the range is high and dense preventing the humidity access from the Pacific Ocean. As a result, atmospheric flow is dominated by the South Atlantic High and winds prevail from the northeast. An intermittent low pressure system, whose likely origin is a combination of thermal and dynamical effects, is located between 20º and 30ºS, in a dry and relatively high area east of the Andes. This system is observed throughout the year, but it is deeper in summer than in winter. When this low is present, northerly flow is favored at low levels over the subtropical region. Therefore, the water vapor entering at low levels comes either from the tropical continent or from the Atlantic Ocean. In the first case, the easterly low-level flow at low latitudes is channeled towards the south between the Bolivian Plateau and the Brazilian Planalto, advecting warm and humid air to southern Brazil, Paraguay, Uruguay and subtropical Argentina. South of 40ºS, the mean flow is from the west during all months and there are intermittent interruptions of polar fronts from the southwest associated with the displacement of Rossby waves over the Pacific ocean [1]. Storms occur frequently and erosion is one of the main features of the region.

The Argentinean Patagonia region is located between 30° and 55°S, where the wind circulation is predominantly westerly all year round, being more intense during winter. As a consequence of the interaction between wind patterns and orography, maximum precipitation (approximately 1600 mm/year in northern Patagonia) occurs in the vicinity of the mountains; decreasing eastward over Patagonian region especially in winter [2, 3] to a low of 300-500 mm/year. Consequently, eastern Patagonia is arid to semi-arid with hydrographic network that begins

generally in the Andes Mountains and flows towards the Atlantic Ocean. Important rivers include the Negro, the Neuquen and the Limay river basins. The most favorable conditions for precipitation in the Patagonian Mountains and its eastern slopes are stationary fronts especially when the cold side of the anticyclone brings moist winds from the Atlantic. The result is stratiform clouds and extended rainfall. In few cases, rainfall occurs due to blocking high pressure systems located in Patagonia or the adjacent Atlantic resulting in extended periods with cloudiness and precipitation.

Neither the spatial nor temporal variability of rainfall in Patagonia have been widely studied, probably due to the limited amount of data that exists in this sparsely populated area with few measuring stations. Using linear regression adjustment to annual rainfall for the period 1950-1999, Castañeda and González [4] detected positive trends with 95% significance level on the order of about 2,5 mm/year in the northern and 1,23 mm/year in southern Patagonia, while precipitation decreased in the western and central zones. The authors used an alternative nonlinear methodology to detect a number of statistically significant breakpoints in order to identify homogeneous periods of stationary rainfall. This method is based on adjusting the data with consecutive linear segments, between periods with significant trends. Their results show that northeastern Patagonia experienced an abrupt change in the mean annual rainfall in the mid-to late 1960s. In the northwest, however, this change occurred later, in the mid-to late 1970s. Barros and Mattio [5] and Barros and Rodriguez Sero [6] analyzed long-term changes in the precipitation over the northern plateau of the Patagonia, especially during the 1940's. They found positive annual rainfall anomalies in northern and central Patagonia (Chubut province) especially in the 1940s and near the Andes Mountains in central Patagonia during the period 1920-1965. However, they detected negative annual rainfall anomalies in southern Patagonia (South of Santa Cruz province) in the 1950s. Minetti et al [7] performed an analysis of nonlinear trends in precipitation over Argentina and Chile using polynomial functions and spectral estimations. They showed that increasing quasi-linear trends were encountered all over Patagonia in the last century with no sign of stabilization in the average value while west of the Andes, in Chile, decreasing trends were observed. Other authors have studied sub-regions within Patagonia. For example, Russian et al [8] studied the relationship between interannual rainfall variability in Northern Patagonia, and tropospheric circulation. The authors detected statistical significant (α=0,05) connections with El Niño/Southern Oscillation (ENSO) and Southern Annular Mode (SAM).

In contrast, the Comahue region, in northwestern Patagonia has been extensively studied because of the economic significance of the hydroelectric power stations operating in the region. Gonzalez and Vera [9] and Gonzalez et al [10] analyzed the connection between Comahue annual rainfall amounts and circulation patterns. The analysis for the Limay River Basin showed that the most important source of predictability came from the interannual variability of surface temperature in the tropical Indian Ocean and the ENSO phase while in the Neuquen River Basin geopotential heights at low levels in the Pacific Ocean, associated with the Rossby wave train that extend along the South Pacific, resulted in the best indicator of rainfall variability. Gonzalez and Cariaga [11] have developed a scheme prediction for winter and spring rainfall in the Comahue region in order to investigate the association

http://dx.doi.org/10.5772/55494

between rainfall and various circulation patterns. The model showed that sea surface temperature (SST) in the tropical Indian Ocean, the wave train over the Pacific Ocean and the ENSO phase observed in the previous month collectively explain 66,5% of the variability of winter precipitation. A similar model was built for forecasting spring rainfall, showing that the dynamical systems are the main factors that contribute to generate spring precipitation accounting for 30% of spring rainfall variance.

Despite such studies, much remains that is unknown or poorly understood about the interannual rainfall variability in Patagonia. For example, the extent to which SSTs influence the annual rainfall remains unclear. The objective of this study therefore is to better understand the connection between the dynamics of the large scale atmospheric forcing, primarily atmospheric circulation patterns and sea surface temperature (SST) conditions and rainfall in Patagonian region.

Slow variations in the earth's boundary conditions (i.e. sea surface temperature) can influence global atmospheric circulation and thus, precipitation. A warming or cooling of some region of the oceans can act as a remote forcing generating teleconnections. Indeed, the most relevant SST pattern in the Pacific Ocean is the El Niño-Southern Oscillation (ENSO). The SST anomalies in tropical Pacific generate a Rossby wave pattern which propagates meridionally towards the middle-latitudes from the tropical source [12, 13, and 14]. This pattern, called the "Pacific South American Pattern", is described by Mo [1]. Some authors [15, 16], have studied the relation between above normal rainfall and "El Niño" events in northeastern Argentina. The authors found that Southern Brazil presents the strongest average signal in El Niño events. They showed that the general behavior toward opposite signals in the precipitation and circulation anomalies over Southern South America during almost the same periods of the El Niño and La Niña events indicates a large degree of linearity in the response to these events.

Related to SST anomalies but located in the Indian Ocean, is the "Indian Ocean Dipole" (IOD) [17]. A positive IOD period is characterized by cooler than normal water in the tropical eastern Indian Ocean and warmer than normal water in the tropical western Indian Ocean and it has been associated with decreased rainfall in central and southern Australia. For South America, Chan [18] showed that IOD excites a dipolar pattern in rainfall anomalies between subtropical La Plata basin and central Brazil where rainfall is reduced (enhanced) over the latter (former) during austral spring. It is also associated with a Rossby wave pattern extending from the subtropical south Indian Ocean to the subtropical South Atlantic. Liu [19] found evidence for the teleconnection detected between IOD and rainfall in Southern South America using the theory of planetary waves [20] and showed that the energy propagation path of planetary waves is approximately along the path of Rossby wave train, a possible dynamic explanation for such teleconnection pattern.

The relative intensity of the sub-tropical high and sub-polar low belts determines the intensity of westerlies over the Pacific Ocean and this factor highly influences rainfall regime in Patagonia. Another teleconnection that influences Patagonian rainfall is the Antarctic Oscillation, an annular-like pattern called "Southern Annular Mode" (SAM) [21]. The positive phase of the SAM is defined by negative pressure anomalies at high latitudes (higher than 65ºS) combined with wave-like pattern in the middle-latitudes. This feature increases zonal winds,

decreases heat exchange between poles and mid-latitudes and so modifies storm tracks. Previous papers have shown SAM's influence on rainfall variability in some regions of South America. For example, Silvestri and Vera [22] found significant (α=0,05) relation between SAM and rainfall amount in southeastern South America particularly during November and December. The authors found that the AAO influence was particularly strong during winter and late spring although of opposite sign and AAO positive (negative) phases were associated with the intensification of an upper-level anticyclonic (cyclonic) anomaly, weakened (enhanced) moisture convergence and decreased (increased) precipitation over southern South America. Reboita [23] detected a decrease of frontal activity when SAM is in a positive phase. These findings are consistent with the results of other investigators. For example, Zheng and Frederiksen [24] showed that the SAM affects summer rainfall variability in the New Zealand sector. They found New Zealand was drier especially in the South Island, when the 500-hPa height pattern had an anomalous high centered well south of New Zealand, with positive anomalies extending over much of the country. Reason and Rouault [25] showed that wetter (drier) winters in western South Africa occur during the negative (positive) SAM phase. The combined effect of the pressure patterns over the oceans and the SST anomalies in close proximity to the continent is another precipitation forcing. When SST is high, evaporation over the ocean is enhanced and moist onshore winds became intensified. Then, advection of moist air from the Atlantic Ocean intensifies and the air above the continent is more likely to generate precipitation. Moreover, significant SST anomalies over the oceans can modify the trajectories of pressure systems from the west.

The objective of this chapter is to better understand the possible global circulation patterns that influence seasonal precipitation in the Patagonian region of Argentina. A second objective is to determine the relationships between regional patterns, like the surrounding oceans SST or wind circulation and seasonal rainfall. This chapter is organized as follows: Section 2 describes the dataset and the methodology; Section 3 presents the results and section 4 discusses the mayor major findings and conclusions.

2. Data and methodology

Monthly rainfall data at 19 stations in Patagonia for the period 1981-2010 are used in this study. The data are derived from different sources including the National Meteorological Service (SMN) of Argentina, the Secretariat of Hydrology of Argentina (SRH) and Territorial Authority of the Limay, Neuquen and Negro rivers basins (AIC). The area of study is located between 37°S and 55°S and between 72ºW and 63ºW (Figure 1). All the selected stations have less than 20% of missing monthly rainfall data and their quality has been carefully proved. Some techniques were applied with that purpose: we discriminated cases with no precipitation in one month from missing data, no stations have records affected by changes of location and instrumentation. Rainfall greater that percentile 95 was controlled in order to detect outliers. In a consistency check, the monthly time series of observed rainfall at each station was compared with a nearby station, using double mass curve analysis, to see if it was physically or climatologically consistent. Suspicious observations according to inconsistencies were not

http://dx.doi.org/10.5772/55494

considered. Seasonal rainfall is calculated as the accumulated precipitation in summer (December-January-February, DJF), autumn (March-April-May, MAM), winter (June-July-August, JJA) and spring (September-October-November, SON).

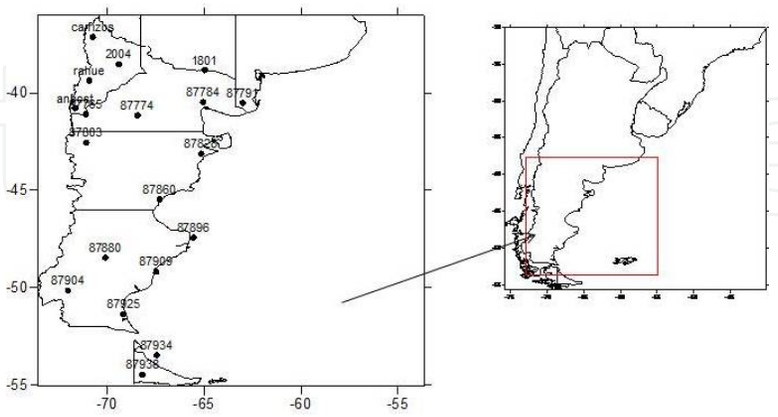

Figure 1. Stations used in the study

The following paragraphs describe the indexes used to analyze the relationship between seasonal rainfall and the different forcings described above.

El Niño-Southern Oscillation effect is evaluated using the mean SST in the EN3.4 region (ENSO) and they are obtained from the Climate Prediction Center (CPC, http://www.cpc.ncep.noaa.gov/products/) from National Oceanic and Atmospheric Administration (NOAA).

The IOD is commonly measured by an index defined as the difference between SST in the western (50°E to 70°E and 10°S to 10°N) and eastern (90°E to 110°E and 10°S to 0°S) equatorial Indian Ocean. The index is called the Dipole Mode Index (DMI) [17]. Data are obtained from SST DMI dataset derived from HadlSST dataset (http://www.jamstec.go.jp/frcgc/research/d1/iod/DATA/dmi_HadISST.txt)

The SAM pattern is represented quantitatively by an index called Antarctic Oscillation (AAO), defined as the difference in the normalized monthly zonal mean sea level pressure between 40ºS and 65ºS [21]. This index is obtained from http://ljp.lasg.ac.cn/dct/page/65572

To analyze the influence of the surrounding Atlantic and Pacific Ocean SST, five indices are defined (figure 2) as: mean SST in (38ºS to 47ºS and 68ºW to 60ºW) (S1), mean SST in (47ºS to 55ºS and 68ºW to 60ºW) (S2), both in Atlantic Ocean; mean SST in (35ºS to 43ºS and 71ºW to 78ºW) (S3), mean SST in (43ºS to 55ºS and 71ºW to 78ºW) (S4) in the Pacific Ocean coast. Finally, mean SST in (55ºS to 70ºS and 78ºW to 60ºW) (S5) in ocean between Argentina and Antarctic is defined.

Additionally, the 500 and 1000 Hpa geopotential height data are used to define the following indices (see also figure 3):

GH1: mean 500 Hpa geopotential height field in (30º to 40ºS and 120ºW to 80ºW) in the South Pacific Ocean, representative of the intensity of sub-tropical high.

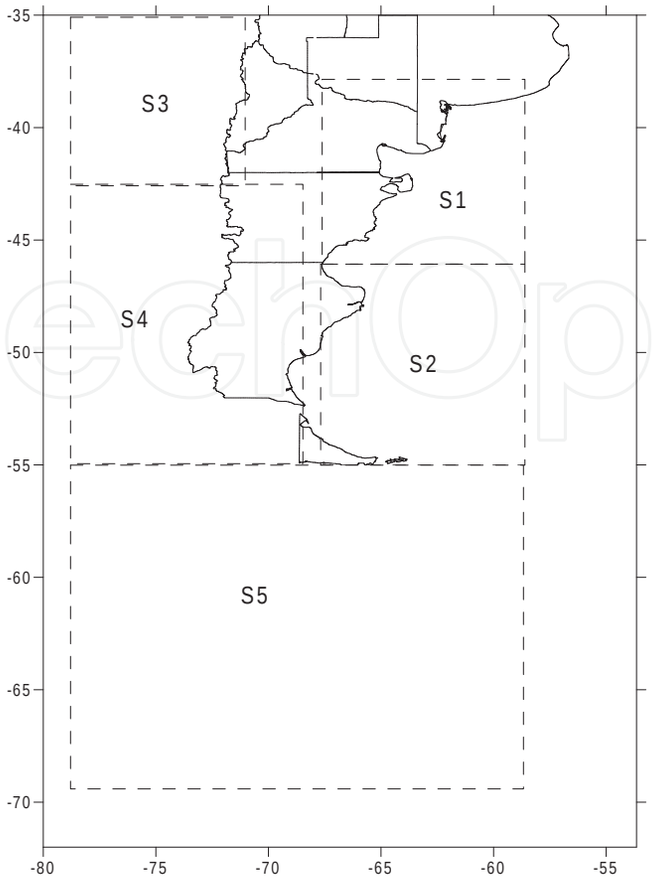

Figure 2. Definition of SST indexes.

GH2: mean 500 Hpa geopotential height field in (60º to 70ºS and 120ºW to 80ºW) in the South Pacific Ocean, representative of the intensity of sub-polar low belt

GH3: mean 500 Hpa geopotential height field in (36º to 55ºS and 65ºW to 55ºW) in the surrounding South Atlantic Ocean

GH4: mean 500 Hpa geopotential height field in (36º to 55ºS and 72ºW to 65ºW) over Patagonian region

GH5: mean 500 Hpa geopotential height field in (36º to 55ºS and 72ºW to 82ºW) in the surrounding South Pacific Ocean

The same indices are defined using 1000 Hpa geopotential heights and the same results are obtained, so they will not be detailed in this paper. SST and geopotential height data are from NCEP reanalysis.

Simultaneous correlations between seasonal (DJF, MAM, JJA and SON) rainfall in the 19 stations and indices defined below (ENSO, AAO, DMI, S1, S2, S3, S4, S5, GH1, GH2, GH3, GH4 and GH5) are calculated. Correlations greater than 0,37 (0,31) are significant at 95% (90%) confidence level. The results are used to describe the relationship between seasonal rainfall and circulation forcing.

http://dx.doi.org/10.5772/55494

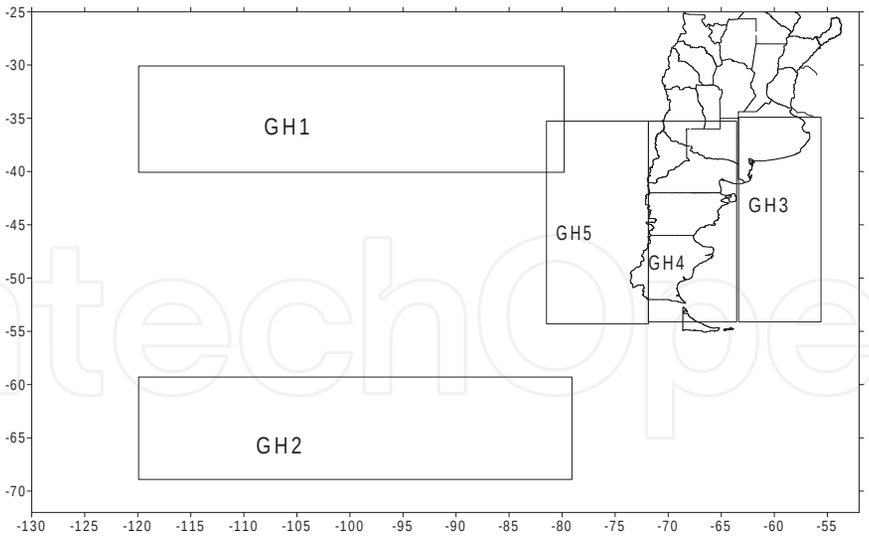

Figure 3. Definition of 500 Hpa Geopotential Height indexes.

The leading patterns of rainfall variability on seasonal time scales were obtained through a Principal Component Analysis (PCA), in the T-mode [26]. Therefore, the principal scores (PC) describe the spatial patterns while the loadings provide the temporal evolution of the patterns. The significant PCs have been detected using the Kaiser criterion [26] in which the eigenvalue must be greater than 1 in order to be considered. The resulting patterns were compared with correlation maps detailed above.

3. Results

The following figures show the correlation fields between seasonal rainfall and all the defined indices. Figures 4 and 5 show simultaneous correlations between JJA rainfall and defined indices. No significant correlations between rainfall and SST are observed. The only exception is a negative significant correlation between JJA rainfall and S5 (figure 4e) is present in a small area in eastern Patagonia, suggesting that cold waters south of the continent could displace systems trajectories towards the north over the continental region. Winter rainfall is increased by the positive phase of ENSO in the eastern of Patagonia (figure 4f). This result agrees with other authors who have investigated the impacts of "El Niño" in South America [14, 15, 16]. Figure 6 shows the temporal pattern of JJA rainfall at station 87860 (located in eastern Patagonia, see figure 1) and ENSO (figure 6a) and S5 (Figure 6b). Figures 5a and 5b show that JJA rainfall is enhanced especially in central and eastern Patagonia, when sub-tropical high and sub-polar lows are weakened (lower sub-tropical high and higher sub-polar low). So, the western flow weakens too and heat exchange between high and middle latitudes increases. This fact facilitates the meridional displacement towards the north of the precipitation systems associated with Rossby waves from the Pacific Ocean [1, 12, 13]. This result agrees with that of Aravena and Luckman [27]. Winter rainfall also increases in the western part of the study region with negative anomalies of geopotential heights over Patagonia (figure 5d) and

surrounding Pacific Ocean (figure 5e), showing the influence of low systems displacing over the continent from the Pacific Ocean. Figure 6c shows the temporal behavior of JJA rainfall in Angostura in northwestern Patagonia (see figure 1) and GH5. Meanwhile, positive anomalies of geopotential heights over Atlantic Ocean coast (figure 5c) tend to increase rainfall in northeastern Patagonia, as indicated by statistically significant (α=0.05) correlation centered on (39ºS; 64ºW), probably because of the increase of moist flow from the Atlantic when an anticyclonic system is present in that ocean.

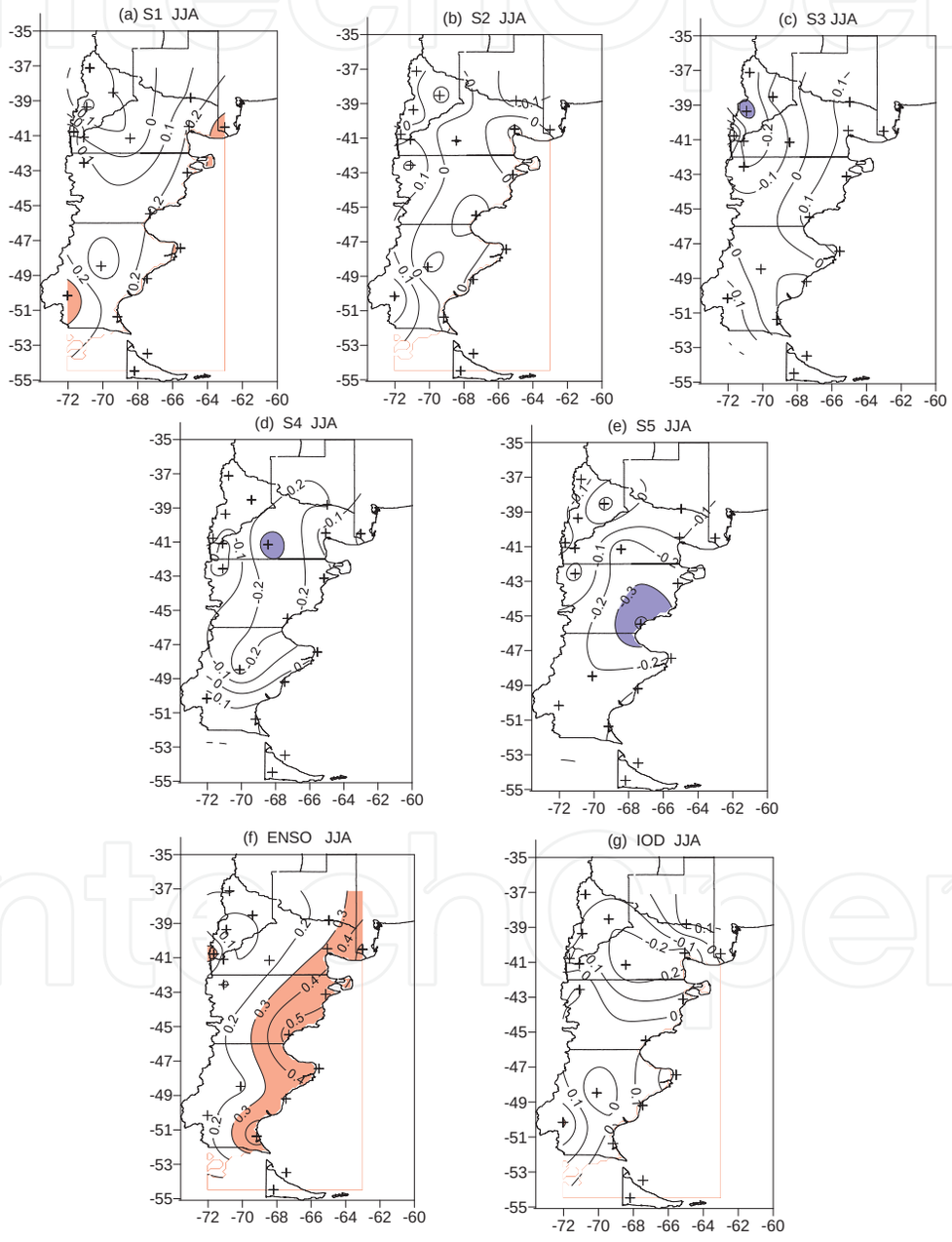

Figure 4. Correlation between JJA rainfall and S1 (a), S2 (b), S3 (c), S4 (d), S5 (e), ENSO (f) and IOD (g) as defined in the text. Areas with positive (negative) significant correlations are red (blue). Correlations greater than 0,31 (0,37) are significant at 90 (95)% confidence level. Stations were plotted.

http://dx.doi.org/10.5772/55494

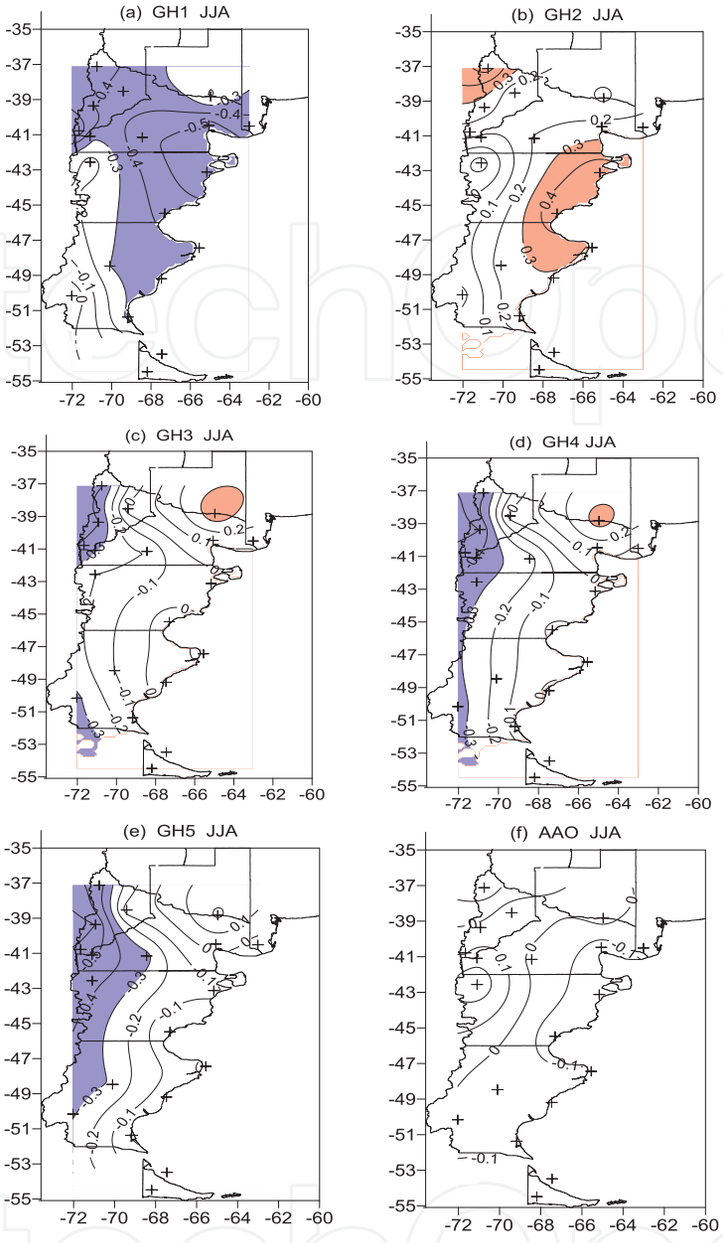

Figure 5. Idem Figure 4 for GH1 (a), GH2 (b), GH (c), GH4 (d), GH5 (e) and AAO (f).

Figures 7 and 8 show simultaneous correlations between SON rainfall and defined indices. The result show that western Patagonia spring rainfall tends to be increased by cold waters in the Atlantic Ocean coast (figure 7 a and 7b) and in the south of the continent (figure 7e). Cold waters over this part of the ocean probably causes systems to displace towards the northeast over the continent as a result of the continental warming which provides the energy necessary for its development. Another factor that influences spring rainfall in northwestern Patagonia is a positive phase of IOD (figure 7g), acting as a source of Rossby waves in the Indian ocean and a warm phase of ENSO (figure 7f). SON rainfall is enhanced by weakened sub-tropical highs (figure 8a) and sub-polar lows (figure 8b) in western and southern Patagonia. This fact implies that rainfall in that area is favored by negative phase of AAO (figure 8f). Besides, more

(a)

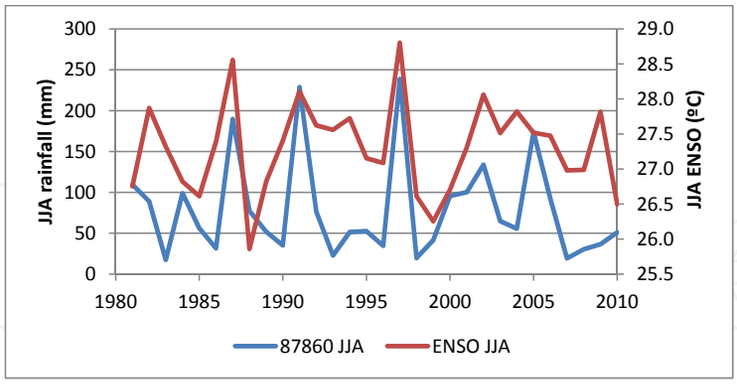

(b)

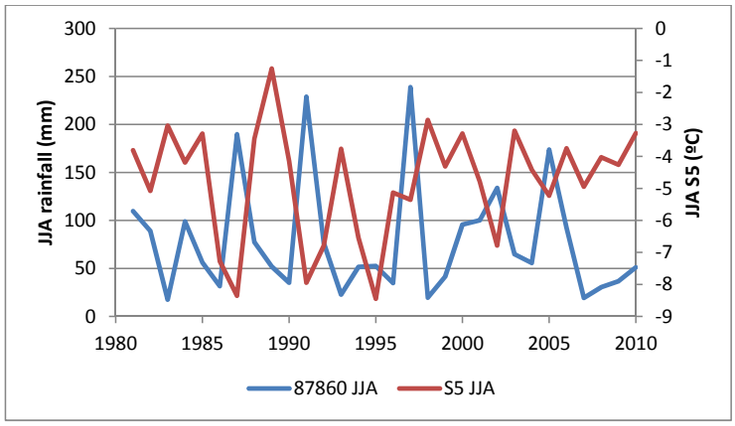

(c)

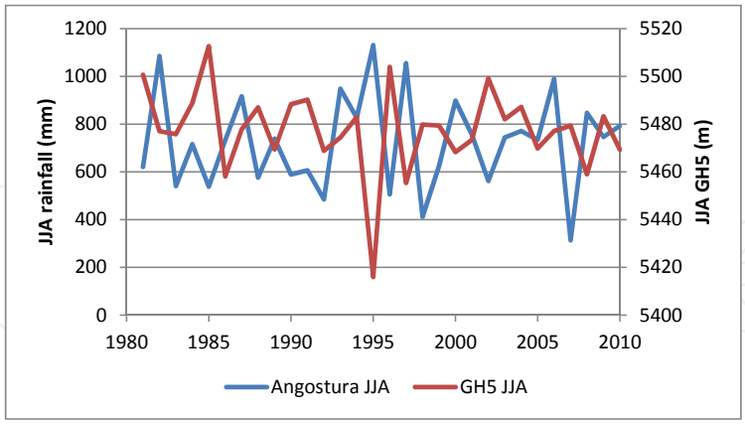

Figure 6. Temporal patterns of (a) JJA rainfall in 87860 station and ENSO, (b) JJA rainfall in 87860 station and S5 and (c) JJA rainfall in Angostura station and GH5.

rainfall is observed when cyclonic anomalies are present over Atlantic (figure 8c) and Pacific (figure 8e) coasts and over the continent (figure 8d). Figure 9 shows temporal patterns of SON rainfall in western Patagonia (87803 station, see figure 1) and ENSO (figure 9a), S5 (figure 9b) and GH5 (figure 9c).

http://dx.doi.org/10.5772/55494

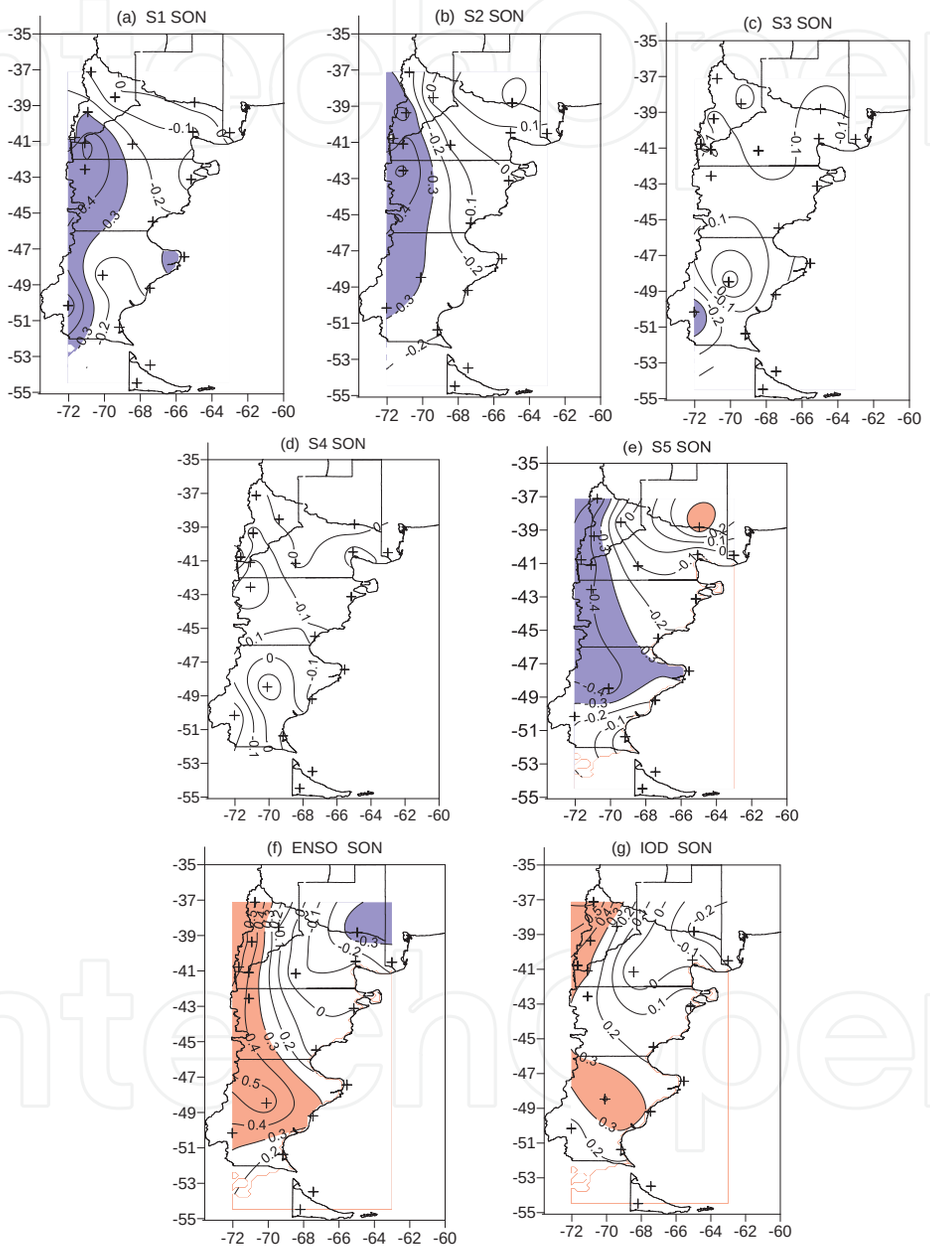

Figure 7. Idem figure 4 for SON.

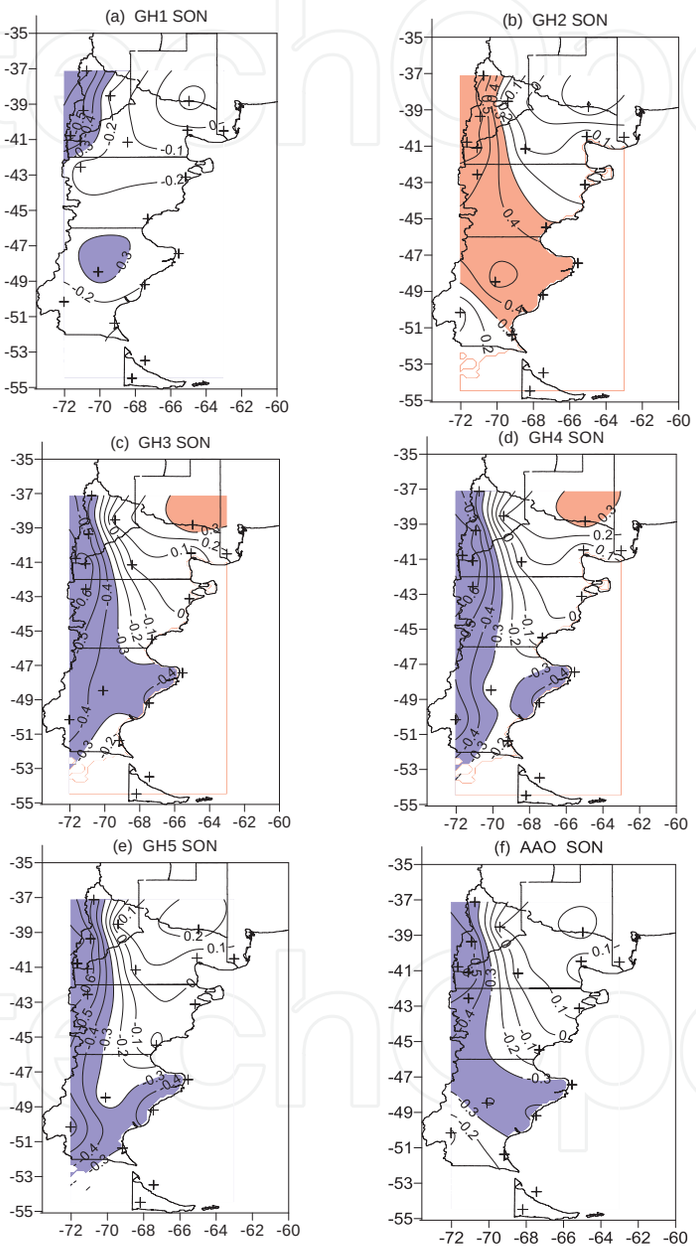

Figure 8. Idem figure 5 for SON.

http://dx.doi.org/10.5772/55494

(a)

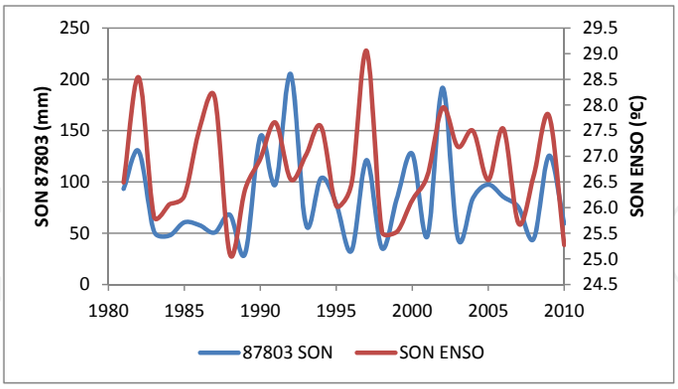

(b)

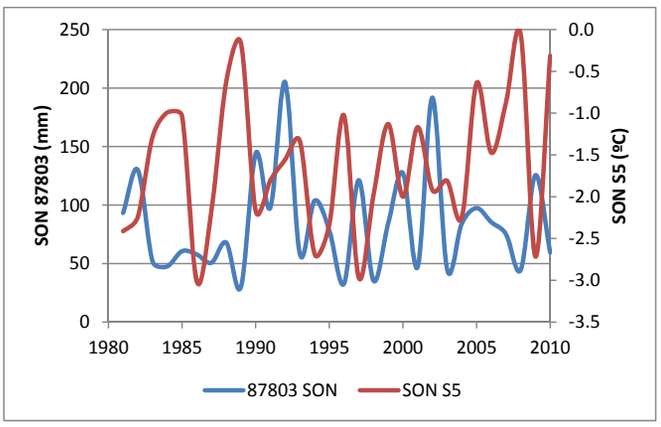

(c)

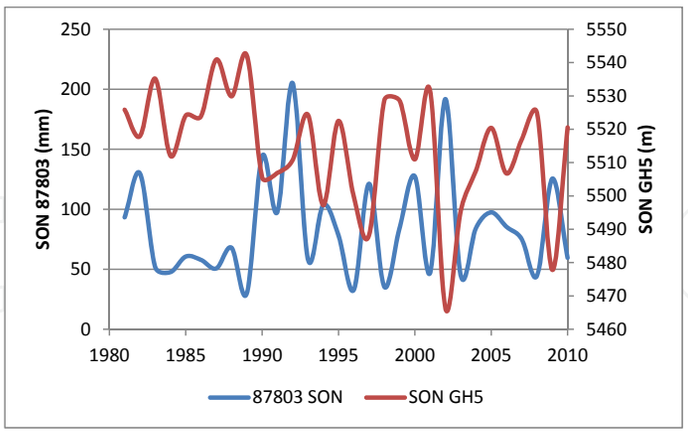

Figure 9. Temporal patterns of SON rainfall in 87803 station and ENSO (a), S5 (b) and GH5 (c).

Figures 10 and 11 show simultaneous correlations between MAM rainfall and defined indices. No significant correlation is detected between rainfall and sea surface temperature in the Atlantic Ocean (figures 10a and 10b). Warm waters in the Pacific coast (figures 10c and 10d) and a positive phase of ENSO (figure 10f) are related to greater than normal autumn rainfall

all over Patagonia. Figure 12a shows the time evolution of MAM rainfall in central Patagonia (87774 station, see figure 1) and S5. As in the case of winter and spring rainfall, weakened sub-tropical highs (figure 11a) and sub-polar lows (figure 11b) and therefore negative phase of AAO (figure 11f) are associated with enhanced rainfall in most of Patagonia. Besides, autumn rainfall in the northwest (Comahue region) is enhanced by cyclonic anomalies in the Atlantic (figure 11c), Pacific (figure 11e) and continental (figure 11d) sectors. Figure 12b shows the temporal pattern of MAM rainfall in northwestern Patagonia (Angostura station, see figure 1) and GH5.

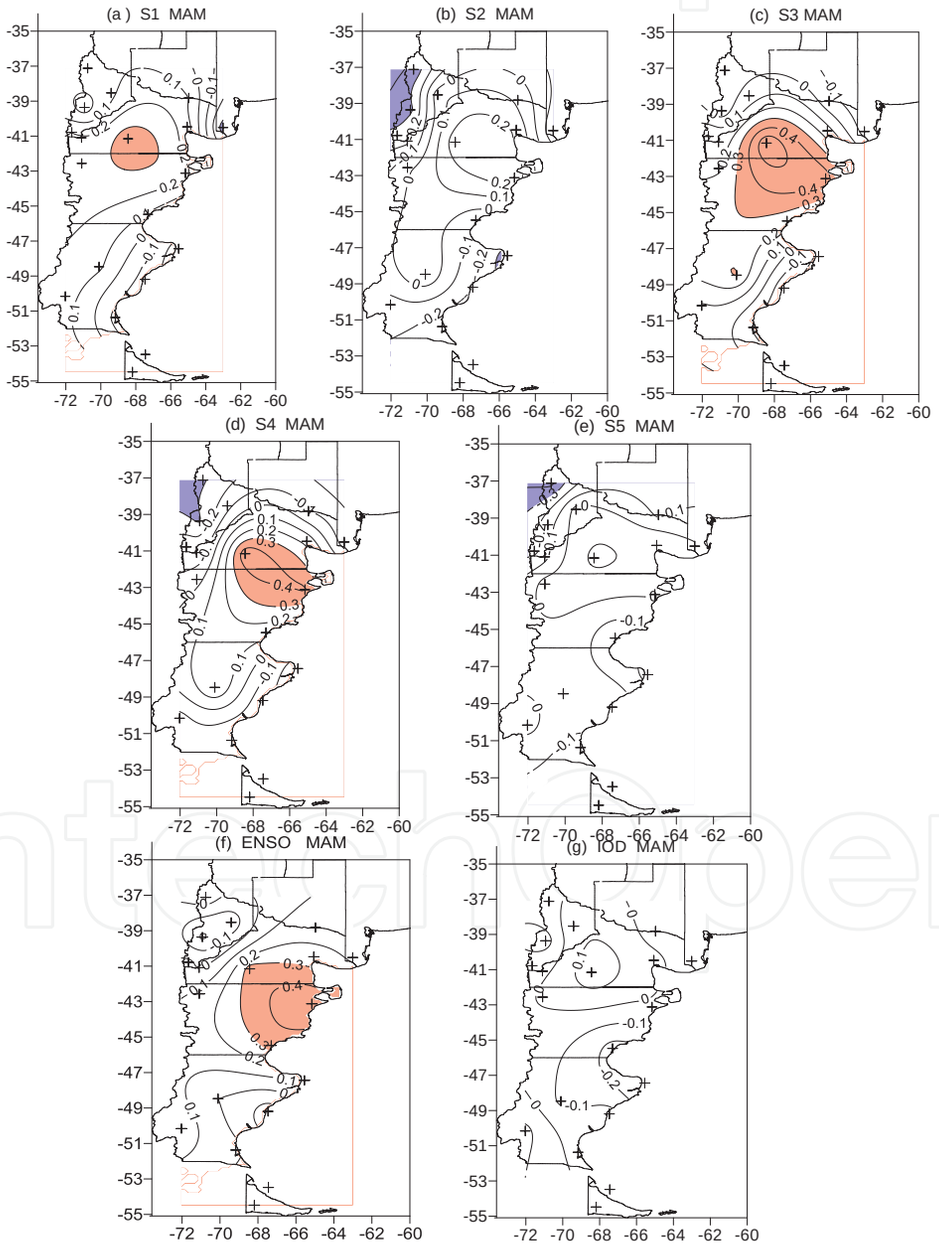

Figure 10. Idem figure 4 for MAM.

http://dx.doi.org/10.5772/55494

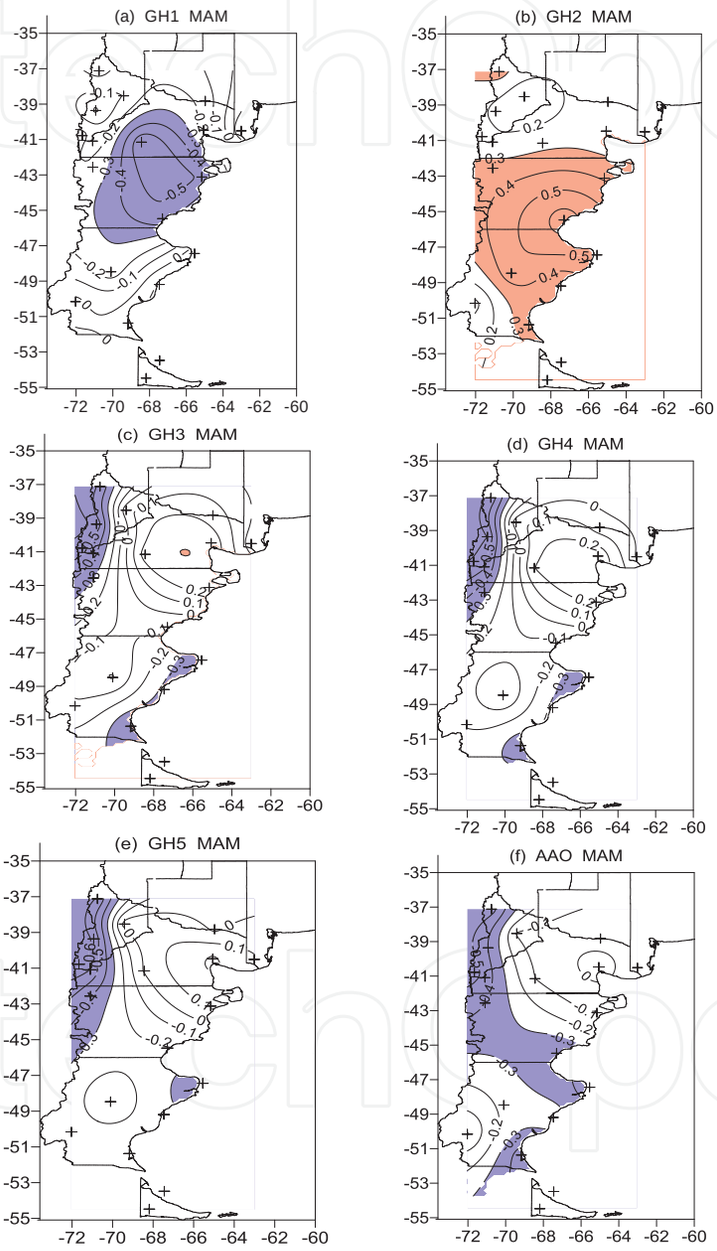

Figure 11. Idem figure 5 for MAM.

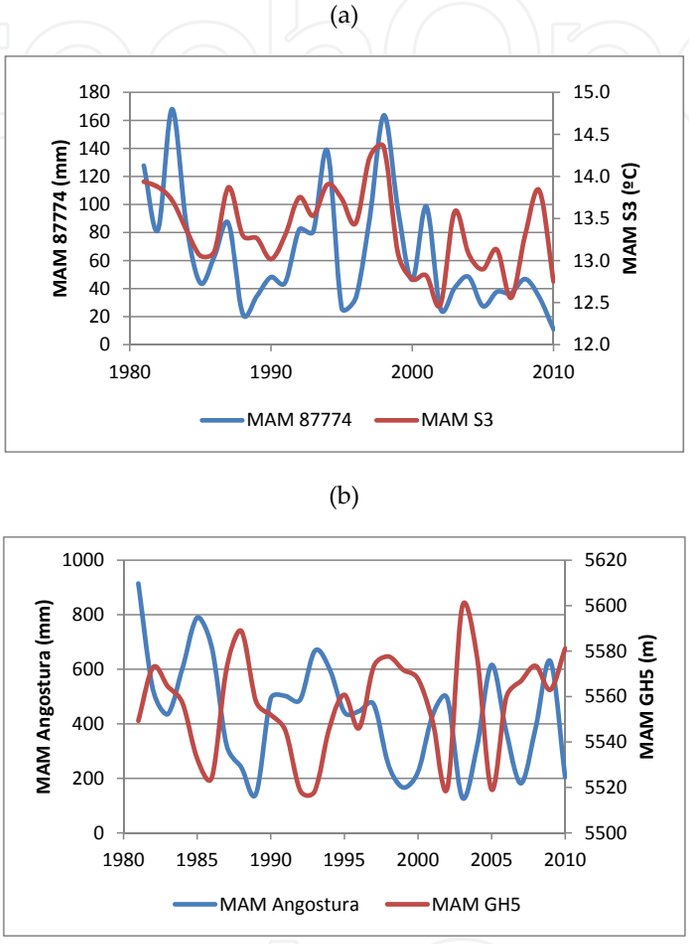

Figure 12. Temporal patterns of (a) MAM rainfall in 87774 station and S3 and (b) MAM rainfall in Angostura station and GH5.

Figures 13 and 14 show simultaneous correlations between DJF rainfall and defined indices. Summer rainfall is very scarce all over Patagonia. No influence is observed between summer precipitation and SST (figure 13). Only cyclonic anomalies over the Atlantic (figure 14c) and Pacific (figure 14e) surrounding oceans and over the continent (figure 14d) are related to enhanced rainfall in the west of Patagonia. Figure 15 shows the time evolution of DJF rainfall in western Patagonia (87803 station, see figure 1) and GH5.

http://dx.doi.org/10.5772/55494

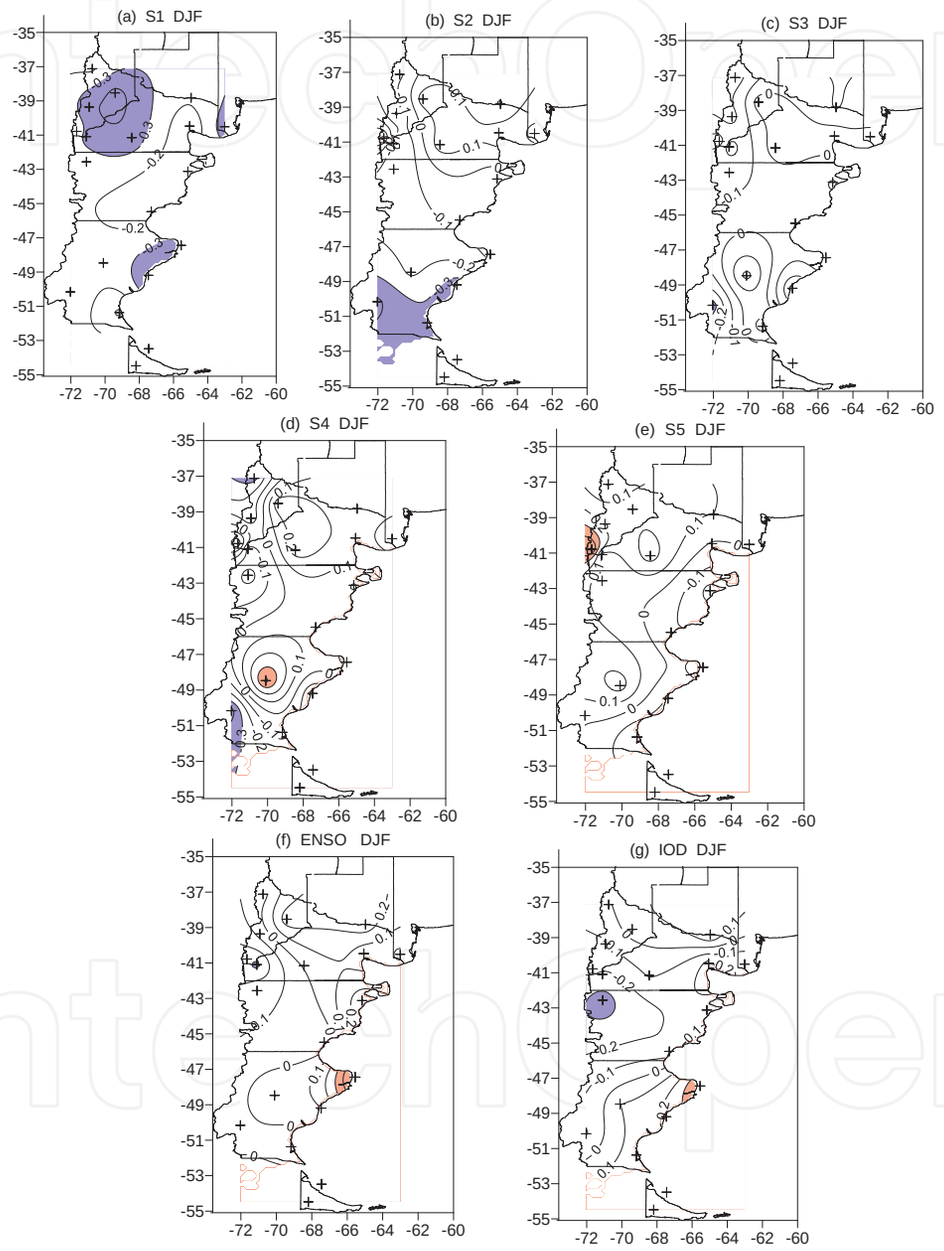

Figure 13. Idem figure 4 for DJF.

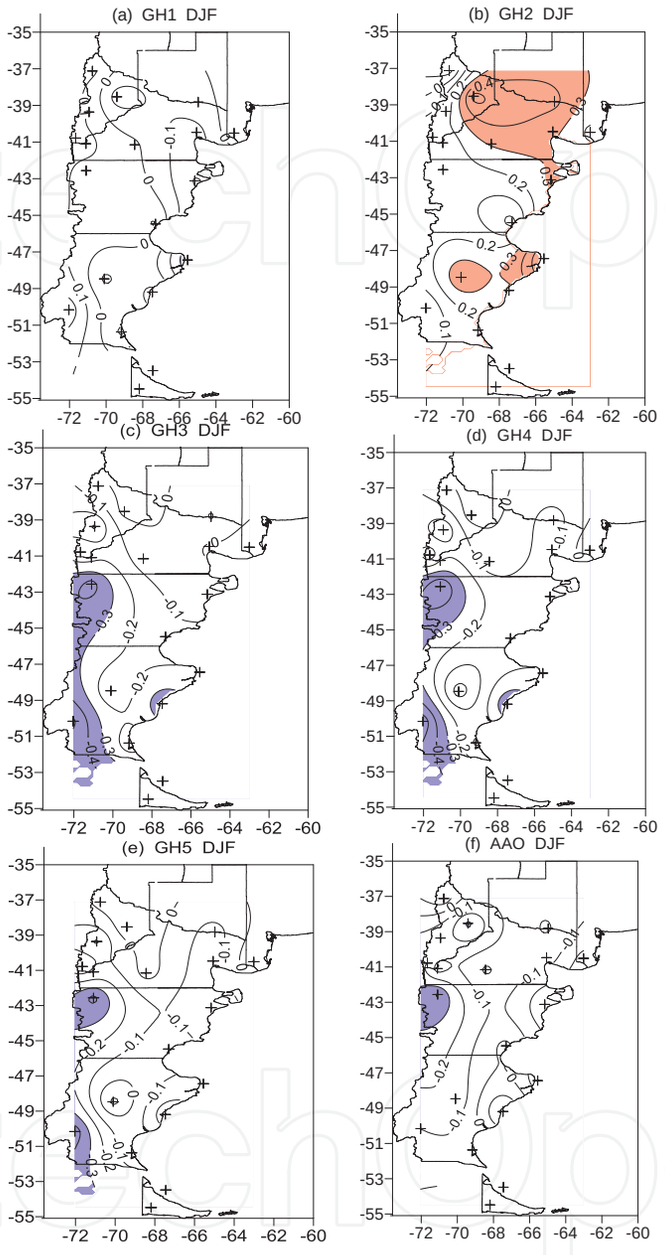

Figure 14. Idem figure 5 for DJF.

In an attempt to reproduce the patterns identified by the indices tested, a PCA analysis was applied to accumulated seasonal rainfall anomalies. The first four spatial patterns of rainfall anomaly are detailed in figures 16 (JJA), 17 (SON), 18 (MAM) and 19 (DJF). Table 1 details the variance explained by each significant pattern. Tables 2, 3, 4 and 5 detailed the correlations between each eigenvector and indices defined in the text for JJA, SON, MAM and DJF, respectively.

http://dx.doi.org/10.5772/55494

Number of loading	JJA	SON	MAM	DJF
1	43,9	39,3	43,6	22,7
2	19,9	15,6	13,2	18,4
3	13,1	10,5	11,1	14,1
4	6,3	7,3	6,3	9,2
5	5	5,8	6,1	8,1
6		4,9	4,2	5,3
7		3,7	3,7	4,8
8				4,1
9				3,5
Total variance explained by significant patterns.	88,2	87,1	88,2	90,1

Table 1. Variance explained by significant loadings (%)

INDICES	Ei 1	Ei 2	Ei 3	Ei 4
EN34	0,135	0,559	0,158	0,086
AAO	0,173	-0,174	-0,014	0,275
IOD	0,420	0,358	0,035	0,247
S1	-0,009	0,197	0,407	0,144
S2	0,109	-0,171	0,317	0,220
S3	-0,274	0,149	0,179	-0,195
S4	0,046	-0,242	0,158	0,034
S5	-0,005	-0,435	-0,119	0,036
GH1	-0,323	-0,435	0,091	-0,163
GH2	0,079	0,499	-0,033	-0,153
GH3	-0,308	0,046	-0,321	-0,201
GH4	-0,403	0,033	-0,351	-0,332
GH5	-0,520	0,009	-0,315	-0,428

Table 2. Correlation between indices defined in the text with the first four temporal patterns (eigenvectors 1, 2, 3 and 4) derived from PCA in JJA. Correlations significant at α=0.05 are shaded.

INDICES	Ei 1	Ei 2	Ei 3	Ei 4
EN34	-0,615	0,238	0,250	-0,271
AAO	0,509	0,055	-0,086	0,046
IOD	-0,432	0,421	0,144	-0,169
S1	0,287	0,135	-0,182	-0,298
S2	0,287	-0,074	-0,337	-0,172
S3	-0,002	-0,103	0,012	-0,364
S4	-0,062	0,000	-0,343	-0,369
S5	0,558	-0,160	-0,332	0,218
GH1	0,559	-0,276	0,064	0,197
GH2	-0,628	0,181	0,084	-0,120
GH3	0,646	0,028	-0,317	-0,121
GH4	0,644	0,011	-0,265	-0,232
GH5	0,665	-0,104	-0,125	-0,282

Table 3. Idem Table 2 for SON

INDICES	Ei 1	Ei 2	Ei 3	Ei 4
EN34	0,038	-0,074	-0,205	-0,383
AAO	0,438	0,110	-0,071	0,334
IOD	0,026	0,020	-0,095	-0,092
S1	-0,217	0,026	-0,272	-0,253
S2	0,244	0,138	-0,168	0,056
S3	-0,123	0,217	-0,261	-0,238
S4	0,212	0,212	-0,103	-0,104
S5	0,181	0,278	-0,044	0,352
GH1	0,208	0,087	0,249	0,403
GH2	-0,144	-0,189	-0,157	-0,399
GH3	0,511	-0,042	-0,149	0,096
GH4	0,596	0,084	-0,105	0,095
GH5	0,679	0,106	-0,009	0,117

Table 4. Idem Table 2 for MAM

http://dx.doi.org/10.5772/55494

INDICES	Ei 1	Ei 2	Ei 3	Ei 4
EN34	0,097	0,280	0,055	0,087
AAO	0,105	0,198	0,224	-0,179
IOD	0,033	0,138	0,330	0,142
S1	0,044	0,002	0,036	-0,237
S2	-0,292	0,098	-0,218	0,144
S3	0,007	0,022	-0,055	0,075
S4	-0,266	0,070	-0,082	0,281
S5	-0,498	-0,068	0,272	0,288
GH1	-0,015	-0,093	-0,018	0,016
GH2	-0,209	0,264	0,021	0,253
GH3	-0,030	-0,013	-0,264	-0,245
GH4	-0,017	-0,113	-0,184	-0,174
GH5	0,017	-0,146	-0,127	-0,114

Table 5. Idem Table 2 for DJF

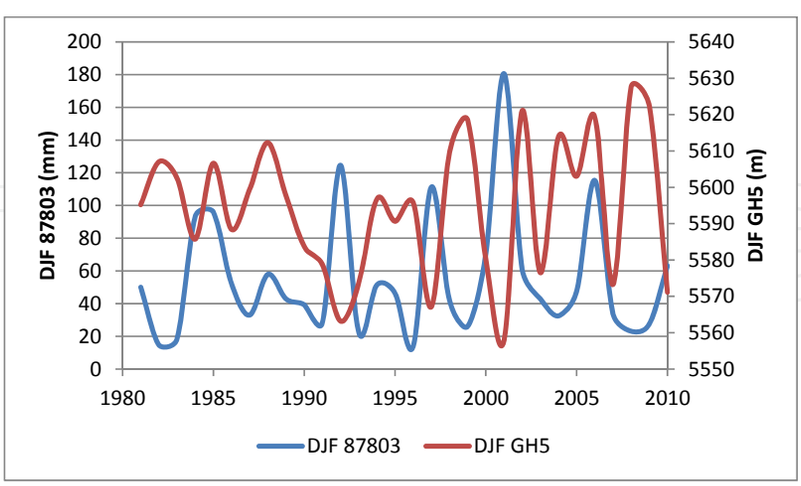

Figure 15. Temporal patterns of DJM rainfall in 87803 station and GH5.

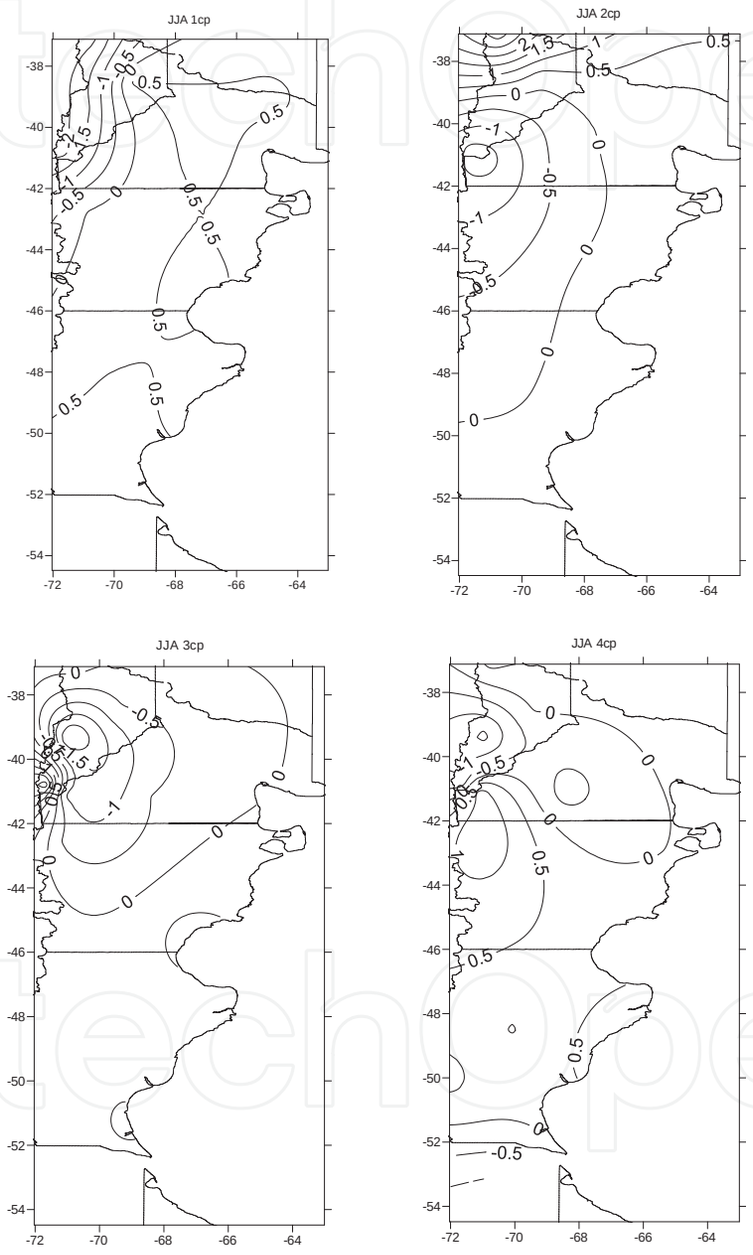

Figure 16. First four spatial patterns of JJA rainfall anomaly derived from CPA analysis during 1981-2010 period.

http://dx.doi.org/10.5772/55494

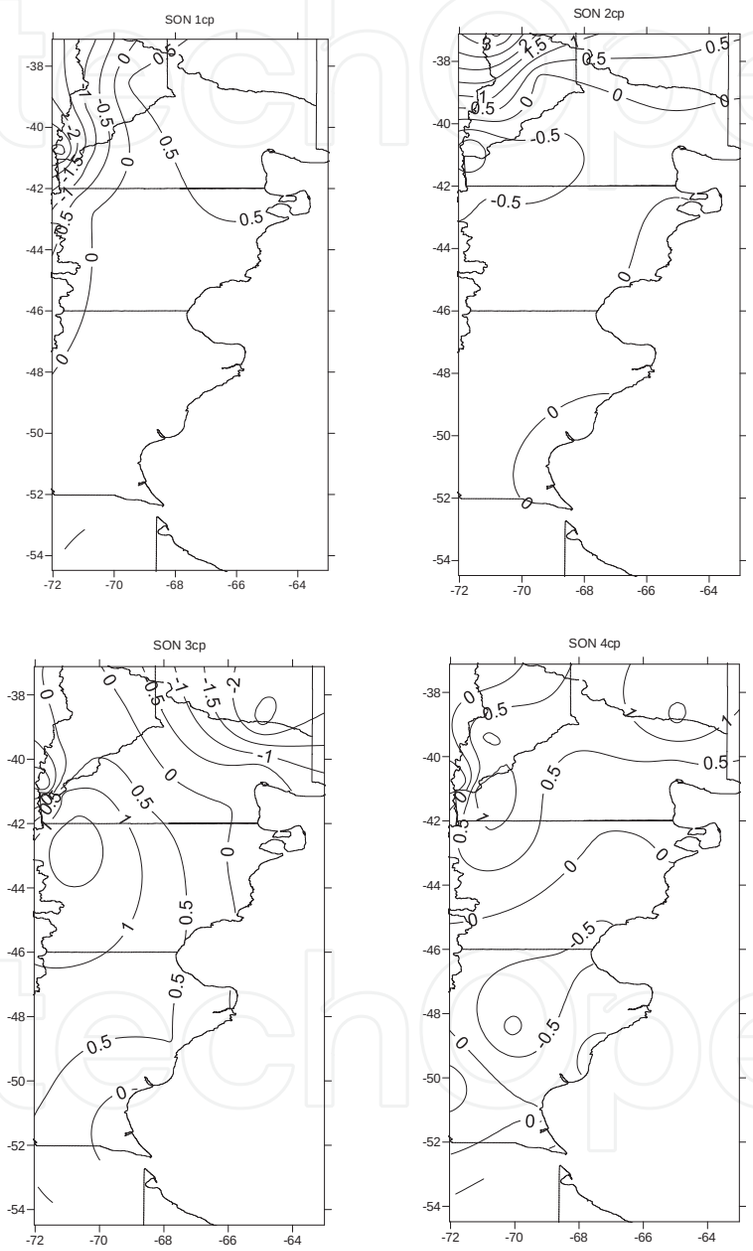

Figure 17. Idem Figure 16 for SON

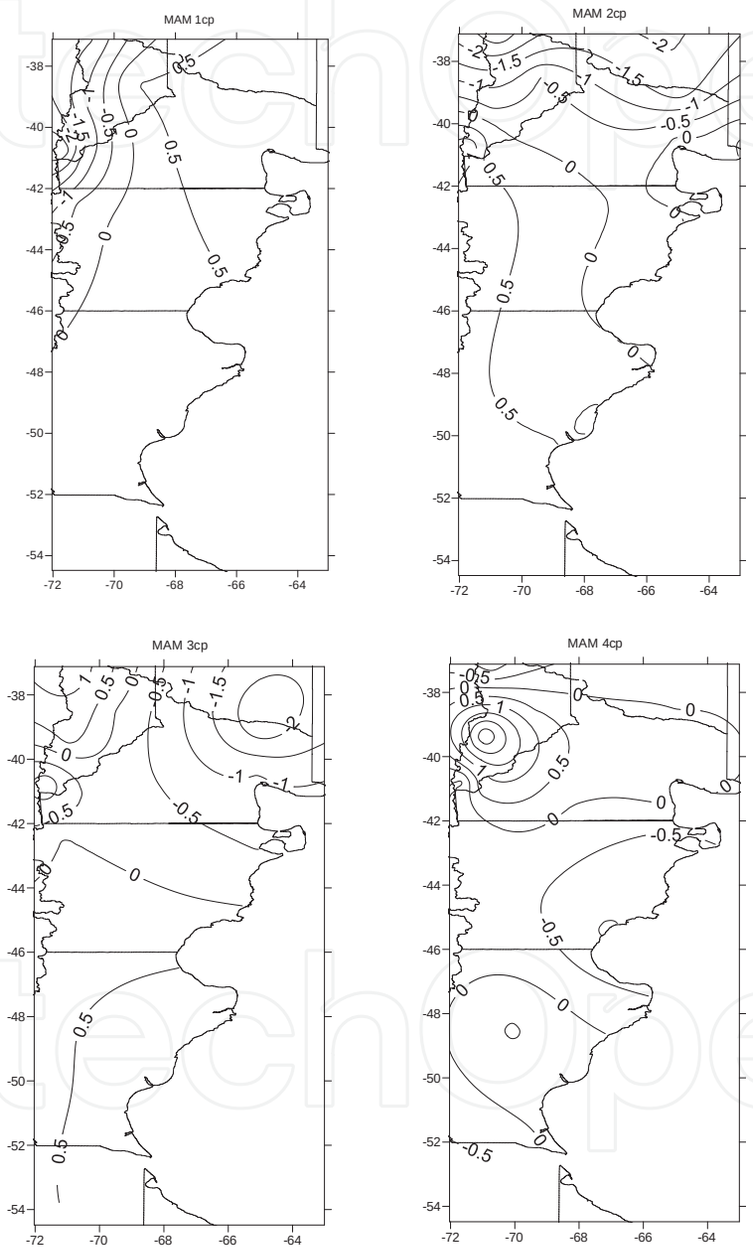

Figure 18. Idem Figure 16 for MAM

http://dx.doi.org/10.5772/55494

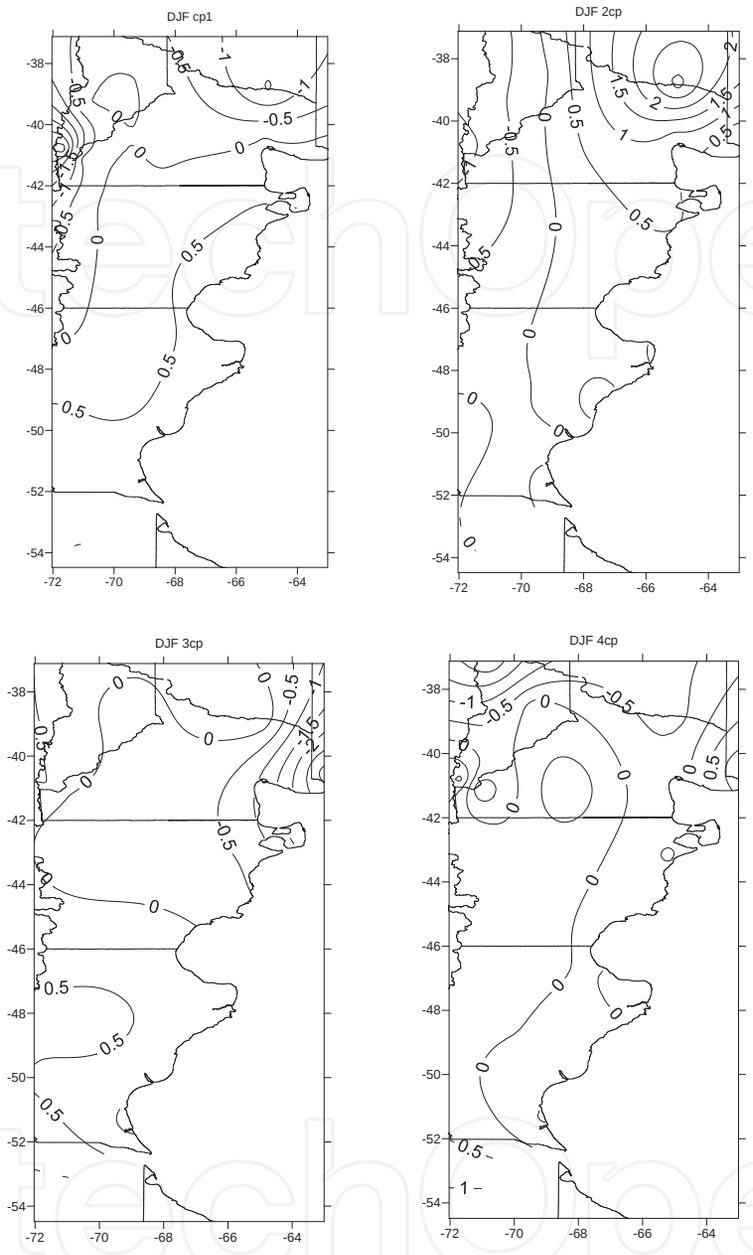

Figure 19. Idem Figure 16 for DJF

Some similarities with the results previously described are detected when the correlations between the eigenvectors and indices are analyzed. In relation to the observed correlations in JJA (Table 2) one can see that the correlation between S5 and the second eigenvector (-0,435) reflects the fact that precipitation increases in eastern Patagonia (Figure 16, JJA 2cp) when S5 is low. Similarly, precipitation increases in this region during the warm phase of ENSO (correlation between ENSO and the second eigenvector 0,559), and when sub-tropical highs (correlation between GH1 and the second eigenvector -0,435) and sub-polar lows (correlation between GH2 and the second eigenvector 0,499) are weaken.

Table 3 shows that in SON, the correlation of the third eigenvector with S2 (-0,337) and S5 (-0,332) reflects the fact that in western Patagonia (Figure 17, 3cp) precipitation increases when S5 and S2 are low. The correlation between IOD and the second eigenvector (0,421) and the first eigenvector (-0,432) indicates that in western Patagonia (Figure 17, 1cp) and in north-western Patagonia (Figure 17, 2cp) precipitation decreases during negative phase IOD. Also the correlation between AAO and the first eigenvector (0,509) also indicates enhanced precipitation in western Patagonia during negative phase of AAO. Sub-tropical highs (correlation between GH1 and the first eigenvector 0,559) and the sub-polar lows (correlation between GH2 and the first eigenvector -0,628) weaken and during the positive phase of ENSO (correlation between first eigenvector and ENSO -0,615), indicate an increase in precipitation in western Patagonia (figure 17, 1CP).

Table 4 shows that the correlation between fourth eigenvector with AAO in MAM is 0.334 and this indicates that in central-eastern Patagonia (Figure 18, 4CP) enhanced precipitation occurs during the negative phase of AAO. Furthermore, when sub-tropical highs (correlation between GH1 and the fourth eigenvector = 0.403) and the sub-polar lows (correlation between GH2 and the fourth eigenvector = -0.399) weakens, enhanced precipitation occurs in central Patagonia (Figure 18, 4CP).

No significant correlation was found in DJF probably because rainfall is scarce in the Patagonia Plateau and the greatest precipitation occurs in winter, near the Andes Mountains.

The Patagonia region in Argentina is of particular interest and is the source of water for hydropower generation for the national grid, the local subsistence economies, agriculture (fruit production) and mining. This complexity is expressed in social and environmental exploitation processes, inequitable distribution of access-control of natural resources, in population displacement and urban growth. Recent climate studies indicate potential future increase in water stress in Patagonia region in Argentina, which will affect the ecological productivity and ecosystem services [28]. Consequently, it is of particular interest to identify current trends and anticipate future scenarios that might lead to environmental and social conflicts. From a climatic point of view, many authors have studied this issue in the South American region [29,30] and found significant changes in precipitation since the beginning of the century. But there are indications of changes in rainfall trends during the past 30 years in some regions [31]. As low frequency variabilities are fed by individual events that occur every year, there is an urgent need for the study of the interannual variability as well as the potential for predicting seasonal rainfall based on teleconnection indices.

4. Conclusions

This findings reported in this chapter are a preliminary attempts to identify the main circulation patterns related to precipitation variability in the Patagonian region of Argentina. The chapter analyzed the relative significance of the various teleconnections responsible for precipitation variability. The teleconnections analyzed include ENSO, AAO, IOD, geopotential

http://dx.doi.org/10.5772/55494

heights and SST patterns. The principal method of analysis was the correlation and the PCA applied to seasonal rainfall.

The results show that the factors which affect precipitation most highly depend on the season and the region. Cyclonic anomalies over the surrounding Atlantic and Pacific Oceans and over the continent enhance precipitation all over Patagonia and in all seasons, although in winter the Atlantic influence is less. The weakening of sub-tropical hights and sub-polar lows over the Pacific Ocean is associated with above normal precipitation throughout Patagonia in transition seasons (MAM and SON) in the eastern part in winter.

Some influences of the SST patterns are present. Warm phase of ENSO enhances rainfall in eastern Patagonia in autumn and winter and in western and southern Patagonia in spring. Warm water in the Pacific coasts tends to increase rainfall in central and eastern Patagonia in autumn while cold Atlantic coast enhances precipitation in west and south Patagonia in spring. The IOD signal is present only in autumn in the western and southern parts of the study region.

Future analysis will investigate the relative contribution of each forcing to seasonal rainfall but that objective is beyond the scope of this paper.

Acknowledgements

Rainfall data were provided by the Territorial Authority of the Limay, Neuquen and Negro rivers basins (AIC), the National Meteorological Service of Argentina (SMN) and the Secretariat of Hydrology of Argentina (SRH). This research was supported by UBACyT 2010-2012 CC02, UBACyT 2011-2014 01/Y128 and CONICET PIP 112-200801-00195, PICT 2010-2110.

Author details

Marcela Hebe González

Address all correspondence to: gonzalez@cima.fcen.uba.ar

Department of Atmospheric and Oceanic Science - FCEN-University of Buenos Aires, Research Center of Ocean and Atmosphere – CONICET/UBA; UMI-IFAECI/CNRS, CIMA - 2º piso, Pabellón II, Ciudad Universitaria, Ciudad Autónoma de Buenos Aires, Argentina

References

[1] Mo, K. C. Relationships between low frequency variability in the Southern Hemisphere and sea surface temperature anomalies. J. Climate (2000). , 13-3599.

[2] Prohaska, F. J. Climates of Central and South America". In: World Survey of Climatology. Amsterdam: Elsevier Cientific Publishing Company; (1976). , 57-69.

[3] Russian, G, Agosta, E, & Compagnucci, R. H. Variabilidad interanual e interdecádica de la precipitación en la Patagonia norte. Geoacta (2010). , 35-27.

[4] Castañeda, M. E, & González, M. H. Some aspects related to precipitation variability in the Patagonia region in Southern South America. Atmósfera (2008). , 21(3), 303-317.

[5] Barros, V. R, & Mattio, H. F. Tendencias y fluctuaciones en las precipitaciones de la región patagónica. Meteorológica (1978). VIII-IX , 237-248.

[6] Barros, V R. and Rodriguez Sero JA. Estudio de las fluctuaciones y tendencias de la precipitación en el Chubut utilizando funciones ortogonales empíricas. GEOACTA (1979). , 10(1), 1979-204.

[7] Minetti, J. L, Vargas, W. M, Poblete, A. G, Acuña, L. R, & Casagrande, G. Non-linear trends and low frequency oscillations in annual precipitation over Argentina and Chile, Atmósfera (2003). , 1931-1999.

[8] Russian, G. F, Agosta, E. A, & Compagnucci, R. H. Circulación troposférica de gran escala asociada a la precipitacion en Patagonia norte. In Proceedings of CONGREMET XI, 28May-1June (2012). Mendoza, Argentina.

[9] González, M. H, & Vera, C. S. On the interannual winter rainfall variability in Southern Andes. International Journal of Climatology (2010). , 30-643.

[10] González, M. H, Skansi, M. M, & Losano, F. A statistical study of seasonal winter rainfall prediction in the Comahue region (Argentine). ATMOSFERA (2010). , 23(3), 277-294.

[11] González, M. H, & Cariaga, M. L. Estimating winter and spring rainfall in the Comahue region (Argentine) using statistical techniques. Advances in Environmental Research (2011). , 11, 103-118.

[12] Kidson, J. Principal modes of southern hemisphere low frequency variability obtained from NCEP-NCAR reanalyses. J. Climate (1999). , 1-1177.

[13] Nogues PaegleJ and Mo, KC. Linkages between Summer Rainfall Variability over South America and Sea Surface Temperature Anomalies. J. Climate (2002). , 15, 1389-1407.

[14] Ropelewski, C, & Halpert, M. Global and Regional scale precipitation patterns associated with El Niño. Mon Wea Rev (1987). , 110-1606.

[15] Grimm, A, Barros, V, & Doyle, M. Climate variability in Southern South America associated with El Niño and La Niña events. J. Climate (2002). , 13-35.

[16] Vera, C, Silvestri, G, Barros, V, & Carril, A. Differences in El Niño response in Southern Hemisphere. J. Climate (2004). , 17-9.

[17] Saji, N. H, Goswami, B. N, Vinayachandran, P. N, & Yamagata, T. A dipole mode in the tropical Indian Ocean. Nature 401; , 360-363.

[18] Chan, S, Behera, S. K, & Yamagata, T. Indian Ocean Dipole influence on South American rainfall. Geophysical Research Letter (2008). L14S12 DOPI: 10.1029/2008GL034204.

[19] Liu, N, Chen, H, & Lu, L. Teleconnection of IOD Signal in the Upper Troposphere over Southern High Latitudes. Journal of Oceanography (2007). , 63, 155-157.

[20] Hoskins, B. J, & Karoly, D. J. The steady linear response of a spherical atmosphere to thermal and orographic forcing. J. Atmos. Sci.(1981). , 38-1179.

[21] Thompson, D. W, & Wallace, J. M. Annular modes in the extratropical circulation. Part I: Month-to-month variability. J. Climate (2000). , 13, 1000-1016.

[22] Silvestri, G, & Vera, C. Antarctic Oscillation signal on precipitation anomalies over southeastern South America. Geophys Res Lett. (2003). , 30-21.

[23] Reboita, M. S, & Ambrizzi, T. and Da Rocha, R. Relationship between the Southern Annular Mode and Southers Hemisphere atmospheric systems. Revista Brasilera de Meteorologia (2009). , 24-1.

[24] Zheng, X, & Frederiksen, C. A study of predictable patterns for seasonal forecasting of New Zealand rainfall. J. Climate (2006). , 19-3320.

[25] Reason, C, & Rouault, M. Links between the Antartic Oscillation and winter rainfall over western South Africa. Geophys Res Lett. (2005). DOI:GL022419.

[26] Green, P. Analysing Multivariate Data. New York: Dryden Press; (1978).

[27] Aravena, J. C, & Luckman, B. H. Spatio-temporal patterns in Southern South America. Int. J. Climatol. (2008). DOI:joc.1761.

[28] Paruelo, J. Valoración de servicios ecosistémicos y planificación del uso del territorio: ¿es necesario hablar de dinero?. In: Laterra P, Jobbagy EG y Paruelo JM (ed.) Expansión e intensificación agrícola en Argentina: Valoración de bienes y servicios ecosistémicos para el ordenamiento territorial. Buenos Aires: INTA; (2012).

[29] Barros, V, Doyle, M, & Camilloni, I. Precipitation trends in southeastern South America: relationship with ENSO phases and the low-level circulation. Theoretical and Appl. Climatology (2008).

[30] Liebmann, B, Vera, C. S, Carvalho, L, Camilloni, I, Hoerling, M, Allured, D, Barros, V, Báez, J, & Bidegain, M. An Observed Trend in Central South American Precipitation. J. Climate (2004). , 17(22), 4357-4367.

[31] González, M. H, Dominguez, D, & Nuñez, M. N. Long term and interannual rainfall variability in Argentinean Chaco plain region. In: Martin O and Roberts T (ed.) Rainfall: Behavior, Forecasting and Distribution. New York: Nova Science Publishers Inc; (2012). , 1-21.

IntechOpen